AD-A092 503 BATTELLE COLUMBUS LABS OH F/G 4/1
COMPARISON OF ELECTRON DENSITIES IN THE MIDDLE ATMOSPHERE INDIC--ETC(U
AUG 80 T M YORK DAAG29-76-D-0100
UNCLASSIFIED ERADCOM/ASL-CR-80-0100-2 NL

1 OF 1
AD A092503

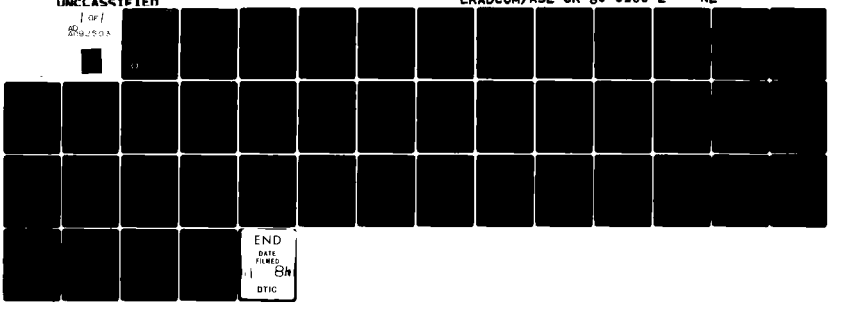

ASL-CR-80-0100-2

COMPARISON OF ELECTRON DENSITIES IN THE MIDDLE ATMOSPHERE INDICATED BY ROCKET BORNE PROBING TECHNIQUES

AUGUST 1980

PREPARED BY

THOMAS M. YORK

Ionosphere Research Laboratory
The Pennsylvania State University
University Park, Pennsylvania 16802

Under Contract DAAG29-76-D-0100

This work was funded under DNA Task
S99QAxAD411 - Reaction Rates to Propagation
Work Unit 23 Variability of D-Region Ion Density and Conductivity

CONTRACT MONITOR: ROBERT O. OLSEN

US Army Electronics Research and Development Command

Atmospheric Sciences Laboratory

White Sands Missile Range, NM 88002

NOTICES

Disclaimers

The findings in this report are not to be construed as an official Department of the Army position, unless so designated by other authorized documents.

The citation of trade names and names of manufacturers in this report is not to be construed as official Government indorsement or approval of commercial products or services referenced herein.

Disposition

Destroy this report when it is no longer needed. Do not return it to the originator.

UNCLASSIFIED

SECURITY CLASSIFICATION OF THIS PAGE (When Data Entered)

REPORT DOCUMENTATION PAGE	READ INSTRUCTIONS BEFORE COMPLETING FORM
1. REPORT NUMBER: ASL-CR-80-0100-2 / 2. GOVT ACCESSION NO.: AD-A092 503	3. RECIPIENT'S CATALOG NUMBER
4. TITLE (and Subtitle): COMPARISON OF ELECTRON DENSITIES IN THE MIDDLE ATMOSPHERE INDICATED BY ROCKET BORNE PROBING TECHNIQUES	5. TYPE OF REPORT & PERIOD COVERED: R&D Final Report 6. PERFORMING ORG. REPORT NUMBER
7. AUTHOR(s): Thomas M. York	8. CONTRACT OR GRANT NUMBER(s): DAAG29-76-D-0100
9. PERFORMING ORGANIZATION NAME AND ADDRESS: Ionosphere Research Laboratory / The Pennsylvania State University / University Park, Pennsylvania 16802	10. PROGRAM ELEMENT, PROJECT, TASK AREA & WORK UNIT NUMBERS: DA Task 1L161102B53A SA2
11. CONTROLLING OFFICE NAME AND ADDRESS: US Army Electronics Research and Development Command / Adelphi, MD 20783	12. REPORT DATE: August 1980 13. NUMBER OF PAGES: 37
14. MONITORING AGENCY NAME & ADDRESS (if different from Controlling Office): Atmospheric Sciences Laboratory / White Sands Missile Range, NM 88002	15. SECURITY CLASS. (of this report): UNCLASSIFIED 15a. DECLASSIFICATION/DOWNGRADING SCHEDULE

16. DISTRIBUTION STATEMENT (of this Report)

Approved for public release; distribution unlimited.

17. DISTRIBUTION STATEMENT (of the abstract entered in Block 20, if different from Report)

Contract Monitor: Robert O. Olsen

18. SUPPLEMENTARY NOTES

19. KEY WORDS (Continue on reverse side if necessary and identify by block number)

D-region
Electron densities
Blunt probe
Middle atmosphere ion collection
Subsonic probe
Electron density probes
Electron collection

20. ABSTRACT (Continue on reverse side if necessary and identify by block number)

Indications of electron density in the middle atmosphere (40-90 km) have been calculated from several different rocket-borne probes, and intercomparisons of these values have been made. Blunt probe data have been analyzed to determine electron densities directly from values of current at positive bias saturation voltages. Saturation currents from subsonic blunt probes are favorably compared with those from supersonic nose tip probes. Supersonic saturation

DD FORM 1 JAN 73 1473 EDITION OF 1 NOV 65 IS OBSOLETE

UNCLASSIFIED

SECURITY CLASSIFICATION OF THIS PAGE (When Data Entered)

20. ABSTRACT (cont)

currents have been analyzed to predict electron densities without any calibration from other diagnostics.

The effects of shock waves or shock compressions have been discussed and included in electron density computations. The related influence of electron attachment on electron density determinations has been evaluated, and it appears that rates higher than those presently accepted are compatible with data. Outgas of water vapor from rocket and probe materials is described, and the amount of outgas near the surface of a probe is evaluated. The influence of water vapor on impedance probe measurements is evaluated for a limiting condition, and in that case is found to be significant.

Comparison of electron density data on one day during the 1979 Canada-US Solar Eclipse Program is made, but close agreement is not evident. This is partially due to the dynamic conditions during the data gathering.

CONTENTS

INTRODUCTION

The determination of electron densities in the middle atmosphere (10-90 km) is important per se because of the impact on communication systems, and indirectly as an important component in the determination of upper atmosphere chemistry.[1,2] The exact specification of n_e in ionosphere models has been a problem for altitudes below 70 km. since most validated diagnostics do not function well with electron densities below 10^3 cm^{-3}.[3,4] There have been a number of reported efforts which involve comparisons of electron density indications in this altitude range from more than one diagnostic with data taken simultaneously.[4-8] However, the results have shown significant differences when the data are reduced by standard analyses. These analyses of diagnostic interactions generally are based on concepts developed in tandem with diagnostic hardware. In many cases, there really has been no controlled verification of a given ionospheric diagnostic technique, so it is not surprising if there are differences evident in predicted composition. In fact, it is the intercomparison of reduced data from diagnostics that will provide the most valuable test of accuracy.[9]

This work will focus on the definition of accuracy and resolution of electron density by a number of different diagnostics. An earlier report[10] had concentrated on the application of a new analysis of electron collection by blunt probes to data which was taken simultaneously with other diagnostics. One set of tests used a partial reflection sounder and other tests used several rocket borne diagnostics. Reasonably good agreement was indicated in these comparisons, but there were differences. One of these differences was accounted for by corrections in number densities derived from WSMR

partial reflection measurements; these were included in a later reporting.[11] The tests that were evaluated were carried out in 1972, 1975 and 1977, while the comparisons in electron density indications were made in 1979--well after the tests. Upon summarizing these intercomparison studies, it became evident that only by conducting experiments with comparisons in mind before the program schedules were set could optimum intercomparison of data be anticipated. The 1979 US-Canada Solar Eclipse Program provided such a campaign within which to conduct needed electron density comparisons. The impetus for an intercomparison effort, and indeed the work being reported here, was generated by R. Olsen of ASL, WSMR. The thrust of the work to be presented here will be directed toward improving the accuracy of analysis of data from a number of probes which were used on that program: blunt probes; nose tip (supersonic) Langmuir probes; impedance probes; and partial reflection sounders. The schedules of a number of rocket firings during the 1979 Solar Eclipse were organized to allow blunt probe and Gerdien probe launches to coincide with those of related impedance probe, tip probe, and spherical particle collector probe launches. This work will be directed to defining the most exact analyses of data from several of these rocket borne probes such that reduction of Solar Eclipse data can be accomplished with the most accurate procedures. Efforts will focus on subsonic blunt probes, supersonic tip Langmuir probes, outgas effects on impedance probes, and shock or compression effects on composition sampled by supersonic probes.

ELECTRON DENSITY DETERMINATION FROM CURRENTS COLLECTED BY SUBSONIC BLUNT PROBES

An earlier study of blunt probe particle collection which resulted in the prediction of electron density profiles,[10,11] exclusively utilized a technique of determining n_e from conductivity, σ_-, which is proportional to dI/dV, the experimentally determined current-voltage slope. As noted in those works, however, it is possible to apply a new analysis[12] of the particle collection to derive electron densities directly from currents collected at specific voltages, for a given probe shape at a given altitude. That technique will be applied here to data that was gathered with two different types of probes: subsonic blunt probes and supersonic nose tip probes with approximately conical shape. As in the earlier work, the indications of electron density that are derived will be compared with those deduced from conductivity and with those from other diagnostics.

For the subsonic blunt probe, several new pieces of information can be added to the present understanding. First, it will be noted that the standard procedure adopted by the Illinois group[4,5] which gathers electron saturation currents by biasing the tip electrode at a constant 2.7 V, is to "calibrate" the probe on a given launch by matching the current to an electron density at one altitude. The variation of electron density with altitude is thus implied by the variation of electron saturation current. As noted in an earlier work, this may have some validity at higher (>70 km) altitudes, but the procedure leads to questionable implications of n_e at lower altitudes because of inter-particle collision effects on collection, along with shock wave and electron reattachment effects. These effects have not been specifically calculated for any such probe.

Again, accepting the fact that tip probe data has traditionally been presented as I_e (current at 2.7 V) and blunt probe data has traditionally been presented as σ_- (dI/dV), it is of interest to evaluate and to graph subsonic blunt probe electron saturation currents to compare with simultaneous supersonic tip probe currents. This comparison has been able to be carried out with data that was gathered by Hale (Penn State University) simultaneously with measurements taken by the Illinois group during the Winter Anomaly campaign. Data was available for January 31, 1972 and December 5, 1972. For the Super Arcas configuration, where a (probe radius)= 3.65 cm, the currents collected by the blunt probe were evaluated at V_p=2 V, and were graphed in the Illinois fashion, i.e., "calibrated" by relating the current to electron density at a given altitude. On Figure 1, data from January 31, 1972 are presented; Illinois data are as published, where the tip probe data are calibrated by the use of Faraday rotation and/or differential absorption rocket-borne techniques. For reference, n_e indications determined from the σ_- reduction are shown. Since currents from the blunt probe at 2 V were not available at altitudes higher than 65 km, the current was "calibrated" to the Illinois current at that point. Based only on the comparison of I_e (blunt) and n_e (σ_-), there are no great disparities in the relative variation with altitude. This same procedure was carried out for the data available from December 5, 1972; this is presented in Figure 2. In this instance, it was possible to "calibrate" the blunt probe current at the highest altitude (74 km) with density from more accurate rocket instruments. Generally speaking, the agreements with Illinois I_e is good from 74 km down to 60 km where it ends. It is worth noting that the unique reversal in n_e at 64 km on this shot is mirrored on both blunt and tip

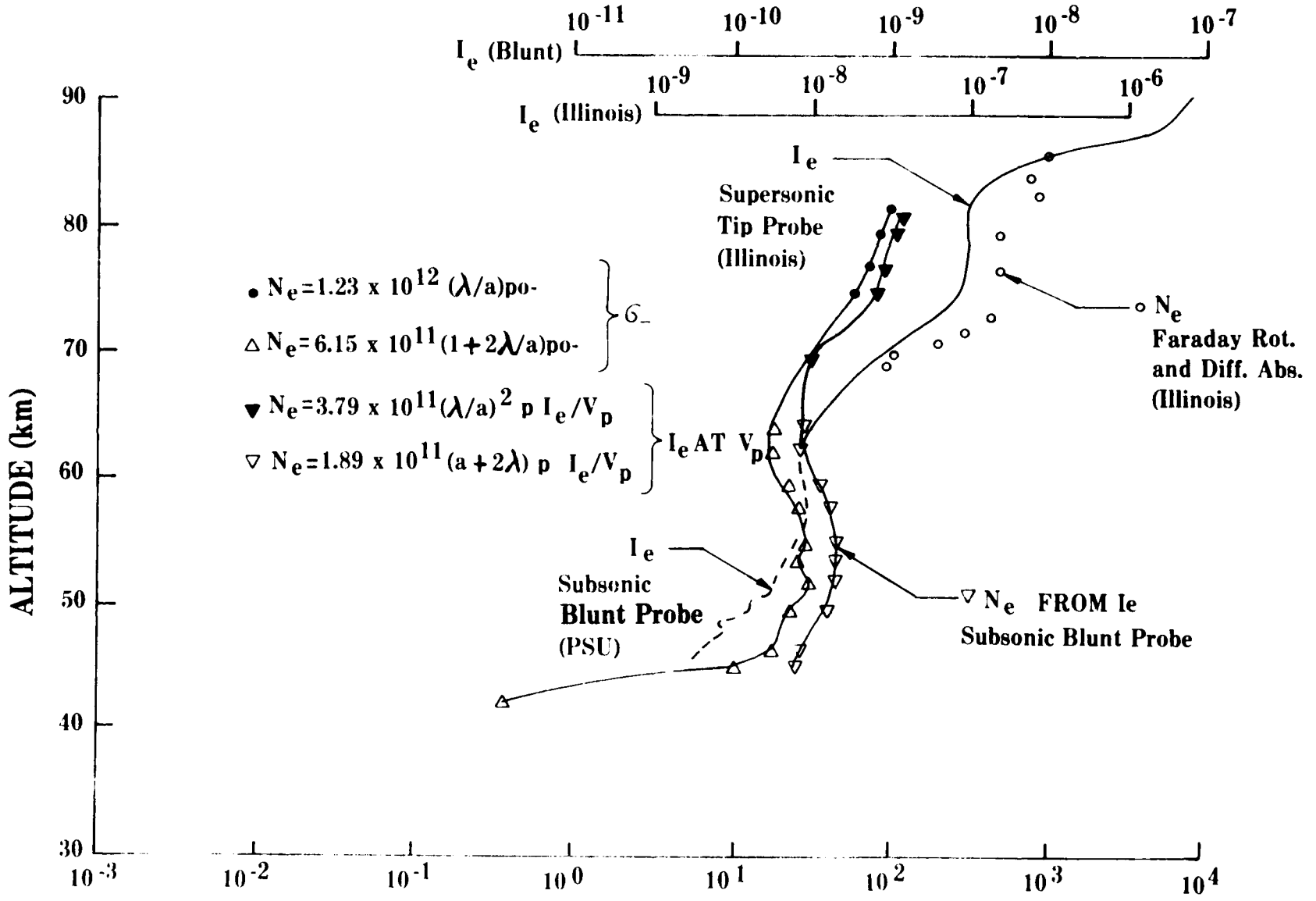

Figure 1. Electron density variations for January 31, 1972, 1230 EST, Wallops Island: blunt probe I_e and calculated densities from I_e, ...

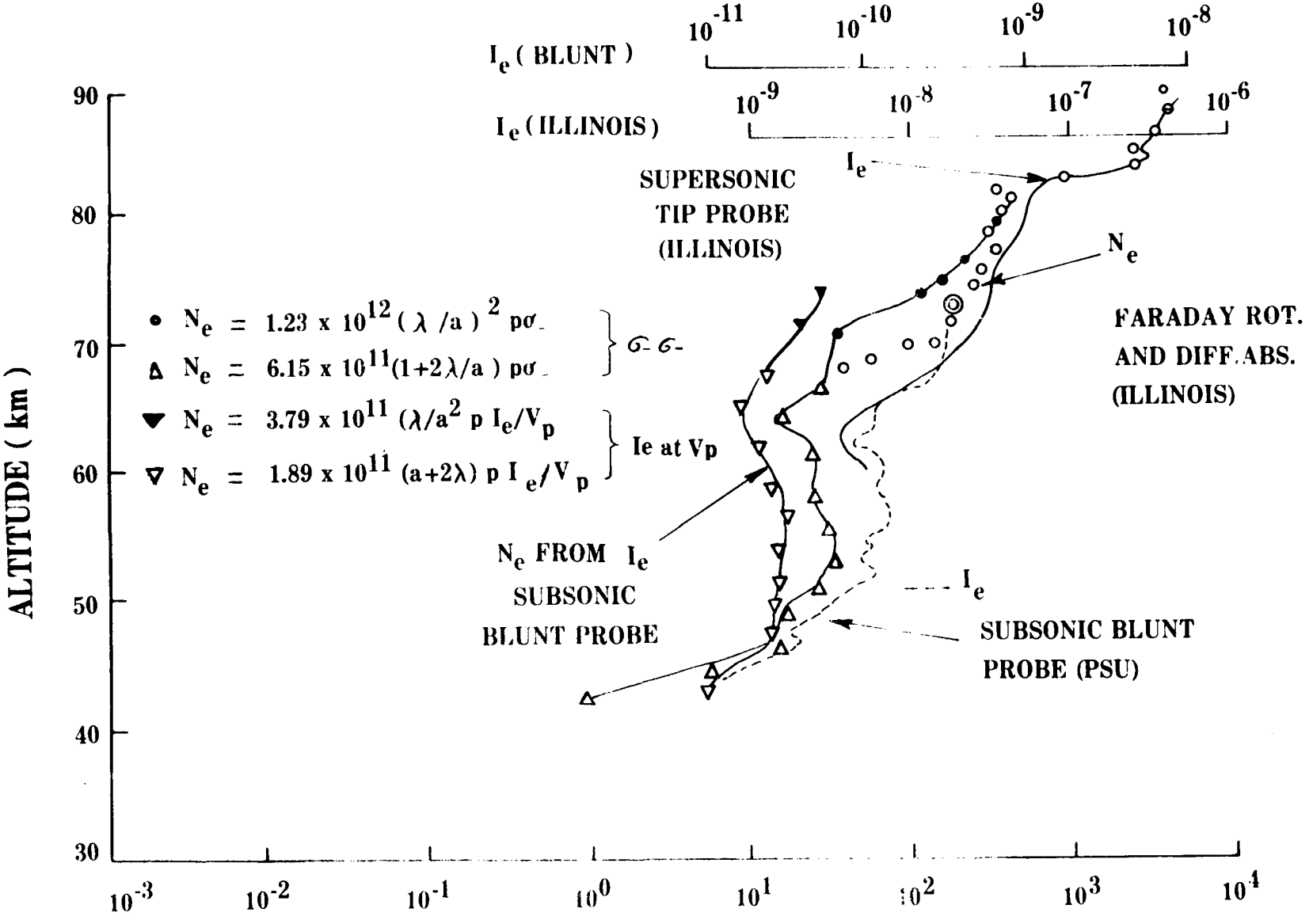

Figure 2. Electron density variations for December 5, 1972, 1210 EST, Wallops Island: blunt probe I_e and calculated densities from I_e, σ.

probes. From the above, it can be concluded that there is little apparent difference of I_e variation provided by supersonic tip probes and subsonic blunt probes at altitudes above 60 km.

With the electron saturation current at a given voltage categorized for the blunt probe, it is now of interest to determine the electron density based on I_e at V_p data. For the blunt probe, this is straightforward, as the relevant equations had already been established.[10,12] For the two days noted above, the appropriate equations and reduced electron densities, n_e, are also presented in Figures 1 and 2. It will be emphasized at this point, that the n_e indications are carried out without <u>any</u> correction or calibration: there is no lateral shift to effect agreement. The n_e values in these figures exhibit the same order of magnitude as those from other diagnostics; the relative variations are also similar. One very interesting aspect of these comparisons can be noted here: for December 5, 1972 the I_e indications are less than σ_- indications of n_e, while for January 31, 1972 the I_e indications are greater than σ_- indication of n_e. One difference between I_e indications and σ_- indications is that I_e can be perturbed by local $\vec{E}$ fields <u>or</u> any variation of vehicle potential from reference potential. Accordingly, such potential or field differences can be evaluated on that basis.

These same procedures can be applied to data taken with a Loki-Dart sized blunt probe, where a (probe radius) = 2.08 cm, at White Sands Missile Range (WSMR) on two different days. As was done earlier, the blunt probe indications of n_e can be compared with partial reflection data. Partial reflection and n_e derived from σ_- can be considered reference data in Figures 3 and 4. Electron current collected with V_p = 2 V is graphed in these figures with a "calibration" point chosen at highest altitude.

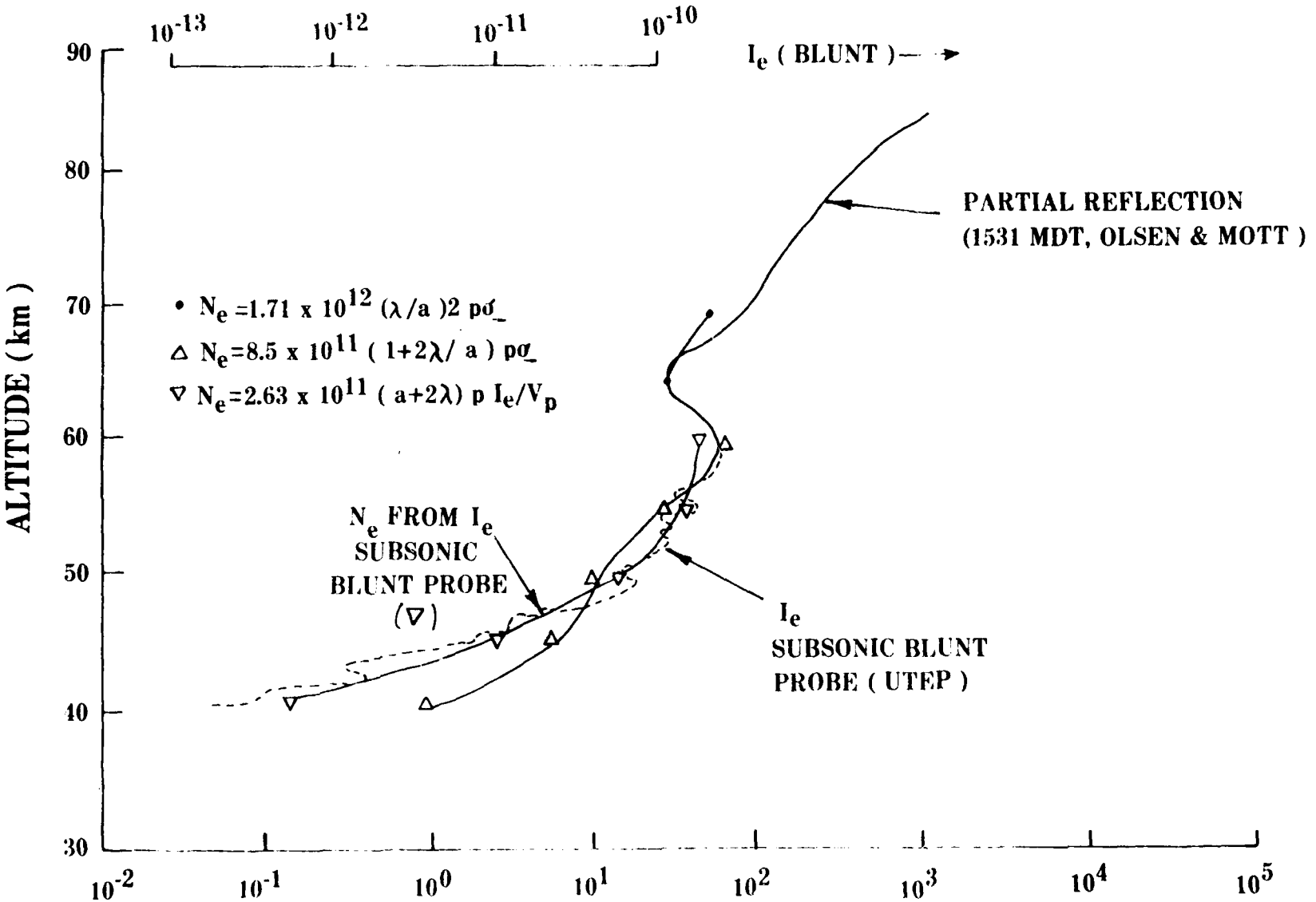

Figure 3. Electron density variations for October 2, 1975, 16[illegible]DT, WSMR: blunt probe I_e and calculated densities from I_e.

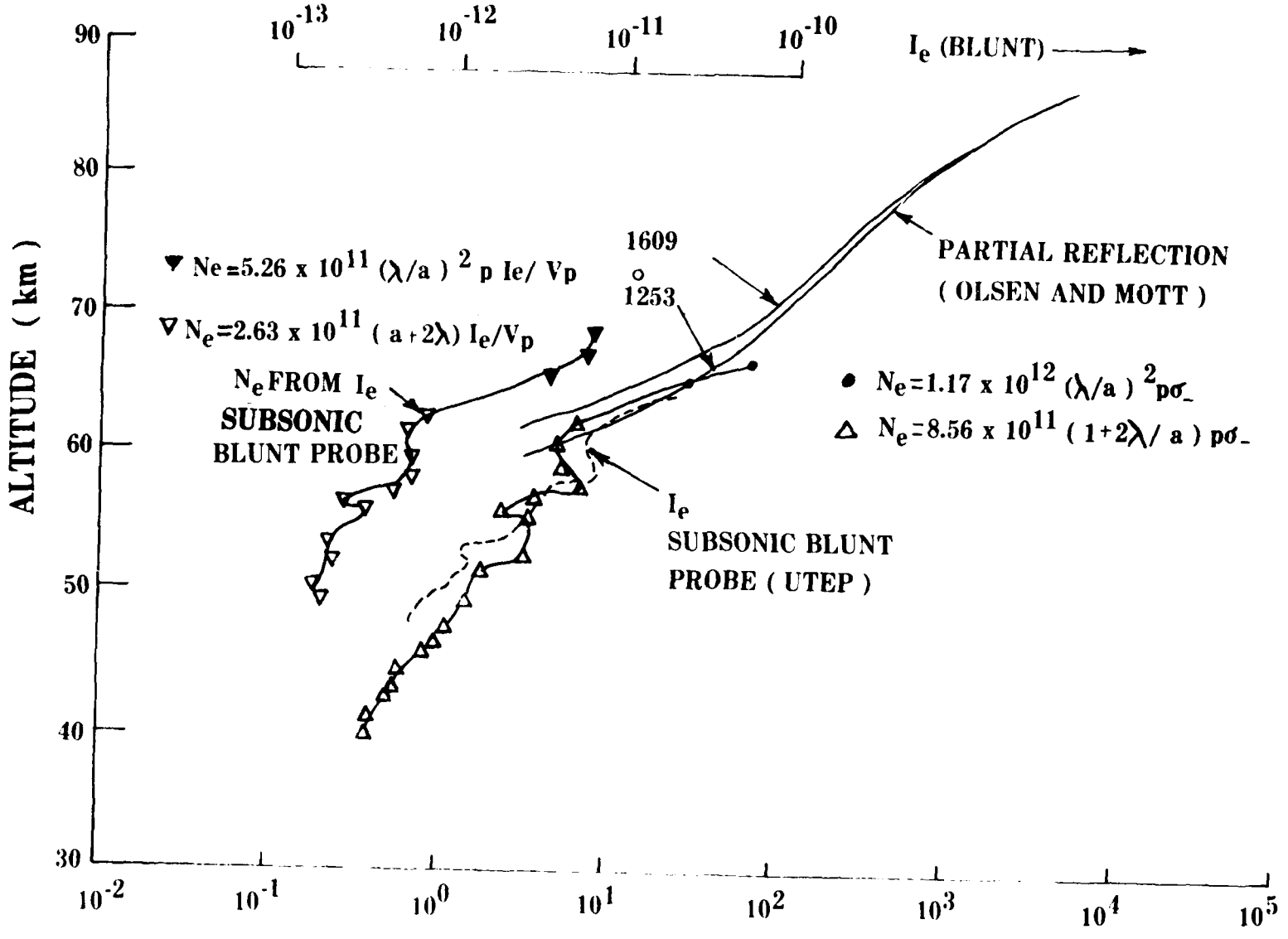

Figure 4. Electron density variations for September 29, 1977, 1345 MST, WSMR: blunt probe I_e and calculated densities from I_e.

Electron densities determined by exact formula, without lateral shaft, are also presented in the figures. As for the data presented from Wallops Island during 1972, there are similar orders of magnitude and variations with altitude from all diagnostic techniques and procedures. Also, as above, the 1977 day shows n_e from I_e below n_e from σ_-, while the 1975 day shows n_e from I_e almost exactly the same as n_e from σ_- for 48-60 km. This, again, could be caused by potential shifts or local field effects.

ELECTRON DENSITIES DETERMINED FROM SUPERSONIC TIP DATA--COMPRESSION AND ELECTRON ATTACHMENT EFFECTS

The above comparisons were based on published information and subsonic blunt probe data which had been shown in an earlier work to be somewhat comparable. However, one of the most important tests of the analysis of data from electron collecting probes must come from different geometry probes, flown by different investigators. Evaluation of such data to determine n_e, and the comparison of n_e with that already presented would be important in establishing the universality of any technique. Fortunately, raw data gathered by the Illinois group using supersonic nose tip Langmuir probes during the 1972 days at Wallops Island were available. This data was retrieved and provided by L. Smith. Also, the detailed geometry of the tip collector was specified as being an ogive with height (base to tip) of 1.5 in., base diameter of 1.082 in. and an arc radius of curvature of 3.209 in. While calculations can be carried out with reasonable accuracy presuming a conical shape instead of an ogival shape, in this work a further approximation was made: the ogive was represented by a hemisphere of equivalent area. A hemisphere of radius 1.42 in. would have equal area with the Illinois ogive.

Following estabiished procedures,[12] the electron flux collected by a hemisphere can be written

$$n_{e\infty} v_{DB} \cdot 2\pi r_B^2 = \frac{1}{4} n_\lambda \bar{c} \cdot 2\pi (r_p + \lambda_{en})^2$$

where $n_{e\infty}$ is the undisturbed electron density, v_{DB} is the saturation velocity at r_B, $r_B = 5\ r_p(Ew/p)$ is the radius for saturation flux, n_λ is the electron density at one mean free path, λ_{en}, from the collector surface, $\bar{c}$ is the electron thermal velocity, and r_p is the radius of the hemispherical collector (probe) surface. Incorporating this into a formulation for current collected by the probe,

$$I_e = e[\frac{1}{4} n_\lambda \bar{c}](2\pi r_p^2)$$

results in the following formula for electron density for $r_p = 1.81$ cm, $V_p = 2.7$ V:

$$n_{e\infty} = (2.72 \times 10^{10}) I_e(A) p(\text{mm Hg}) (1 + \lambda_{en}/r_p)^2$$

When appropriate data were substituted into the above formula, the values of electron densities were calculated in a straightforward manner. These electron densities are indicated in Figures 5 and 6 (by the notation "N_e from Supersonic Tip Probe"); generally these values are higher at higher altitude and lower than other diagnostics at lower altitude. At altitude above 60 km, the rate of change of n_e is in reasonable agreement with that derived from other diagnostics. Before proceeding with further calculations, it should be noted that the analytical formula above is sensitive to the model chosen for A_λ, the collection area at λ from the probe surface. However, using a consistent approach, an alternative approximation with cylindrical shape

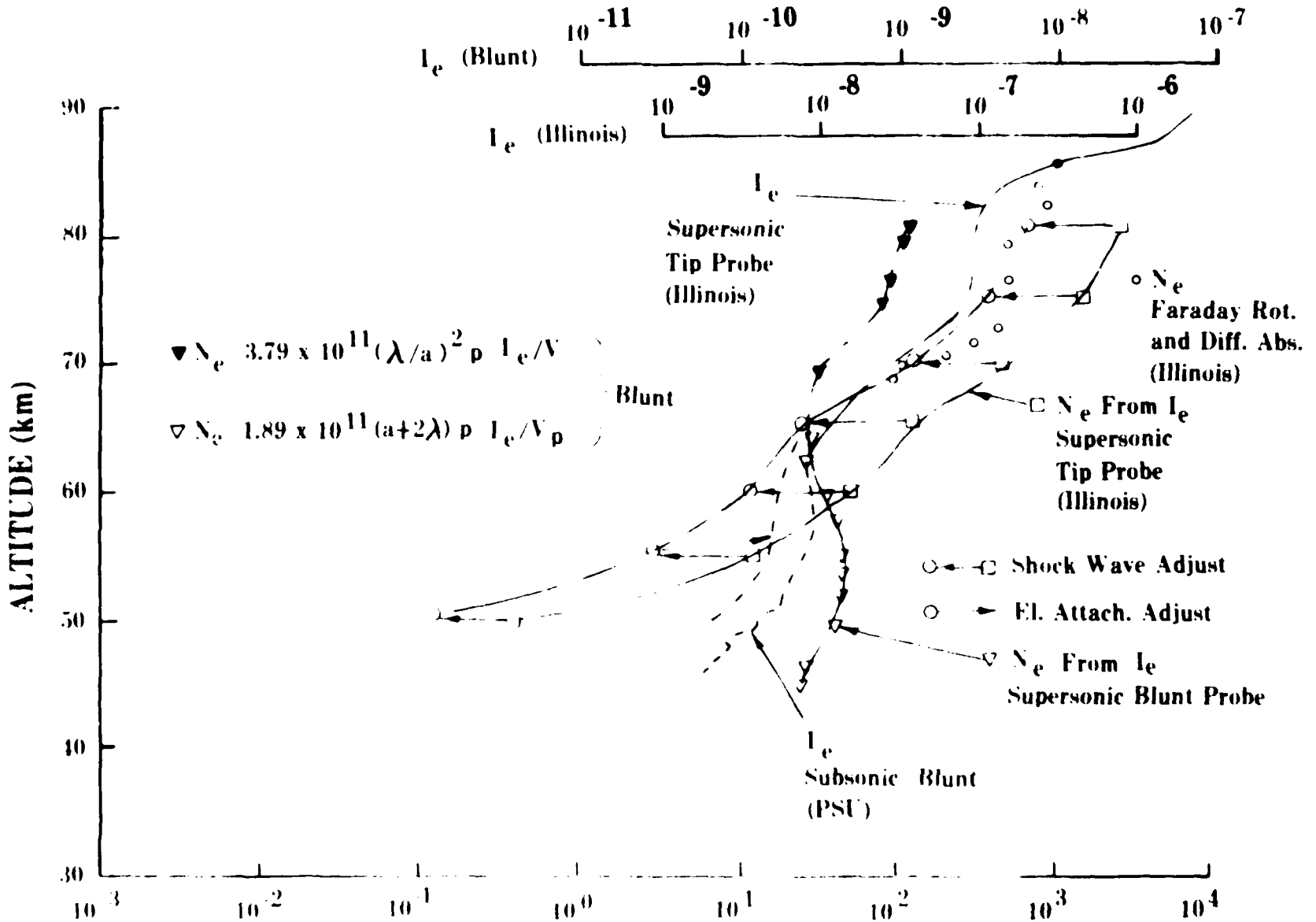

Figure [illegible]. Electron density profiles for January 31, 1972, [illegible] EST, Wallops Island: [illegible] from I_e for [illegible].

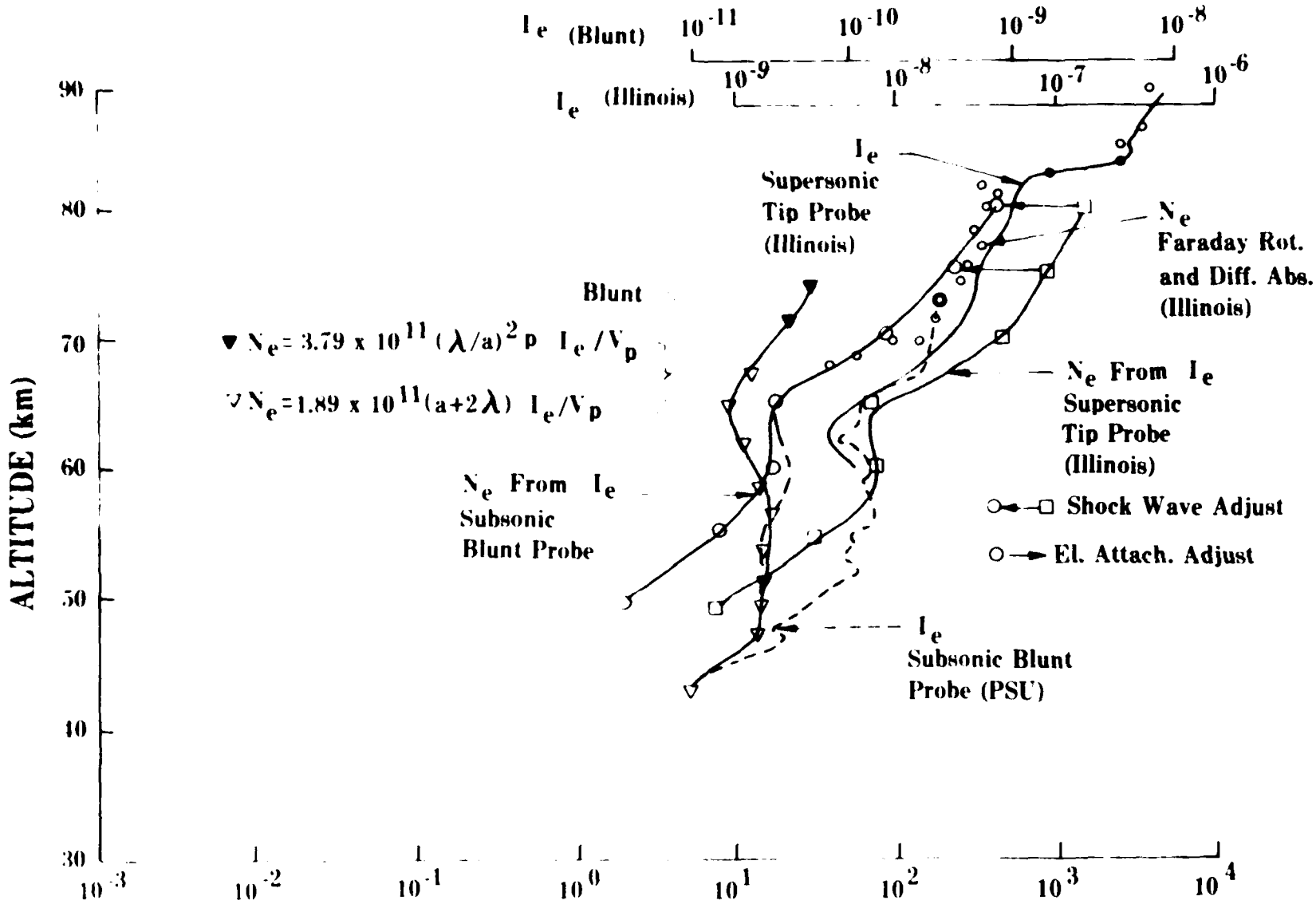

Figure 6. Electron density variations for December 5, 1972, 1230 EST, Wallops Island: tip probe I_e and calculated densities from I_e for comparison.

gave the same numerical results. Accepting the above form as reasonable, further analyses will proceed.

There are two effects that must receive attention in the reduction of supersonic collection data: (1) the compression effects of shock waves about the collecting shape, and (2) the alteration of plasma chemistry by the shock wave event. Both of these effects are dependent upon the vehicle trajectory (Mach number). It will be reiterated that an earlier report identified a number of references which established the magnitude and extent of shock-type compressions up to 100 km. Further, it can be noted that the electron collection processes generate particle flux to the surface at radius, r_B, which is far from the surface; r_B will be well outside any shock or compression region. However, kinetic flux to the surface at $)_{en}$ will be proportionally altered by the shock or compression effects. A simple, linear approach allows the compression effects to be compensated for in a sequential manner. In order to evaluate the magnitude of these two effects on electron density, approximate calculations were carried out. First, based on trajectory information supplied by Illinois, Mach numbers were evaluated as a function of altitude. On January 31, 1972, flight Mach number was about 5.2 for 50-80 km; on December 5, 1972, flight Mach number was about 4.9 for 50-80 km. For the ogive shape used, the half-cone angle of 30° is indicated[13] to result in a shock wave angle of about 35°. By standard procedures, the density ratio across the shock wave is $P_2/P_1 \simeq 4$ and $T_2/T_1 \simeq 2.7$. Directly, this means that the density of particles within the shock cone would be raised by a factor of 4; to recover densities in the ambient medium, it is appropriate to divide the indicated electron densities by this factor of 4. The primary values of electron density noted

above were adjusted first for shock compression effects, and these are noted in Figures 5 and 6 by arrows indicating the adjustment. It can be seen that this calculation procedure results in values that are in very close agreement with those of other diagnostics for altitudes between 80 and 60 km. Below 60 km, the electron densities reduced by including shock compression effects are substantially lower than those derived from subsonic blunt probes.

A second major correction effect to the supersonic nose-tip Langmuir probe data must be considered at lower altitudes. The presence of a strong compression region in front of the collector can result in substantial electron loss through enhanced reattachment of the electrons. Specifically, electron loss mechanisms were reviewed by both Mitchell[14] and Heaps,[15] and the dominance of loss by attachment was identified. The simplest model that can describe attachment is written

$$\frac{dn_e}{dt} \approx - \beta n_e$$

where β is the attachment rate coefficient derived from the two reactions

$$N_2 + O_2 + e^- \rightarrow O_2^- + N_2$$

and

$$O_2 + O_2 + e^- \rightarrow O_2^- + O_2$$

to be

$$\beta = 1.4 \times 10^{-29} \left(\frac{300}{T}\right) e^{-(600/T)} [O_2]^2 + 10^{-31} [O_2][N_2]$$

In the above, [ ] refers to the number density of the species in the parenthesis. Integration of the equation for n_e gives

$$n_e = n_{eo} e^{-\beta t}$$

where n_e is the electron density behind the shock wave after chemical reaction involving incoming flow has taken place while n_{eo} would be the density behind the shock waves presuming no chemical reaction (reattachment). The characteristic time available for reattachment can be evaluated by considering the average speed of particles behind the shock and the average distance traveled before collection;

$$t \simeq d/V \simeq 1 \text{ cm}/10^4 \text{ cm sec}^{-1} \simeq 10^{-4} \text{ sec} .$$

Accordingly, the effects of reattachment are included by using the shock adjusted values of n_e noted above, and appropriate β, t values to calculate n_e. It should also be noted that the value of β that was used is different from that appropriate for ambient conditions, since the shock compression and heating alter the density and temperature values and also β. Further, there is some conjecture regarding the correct attachment rates in the light of available information.[15] Specifically, Heaps[15] notes that attachment rates about two orders of magnitude higher than standard rates are necessary to allow his computational model to be in reasonable agreement with changes noted during an eclipse. In fact, this same type of behavior is consistent with supersonic tip probe data: if an attachment rate is chosen which is a factor of 15 higher than standard, there is good agreement between subsonic shunt probe n_e and supersonic tip probe n_e at all altitudes below 60 km. The appropriate data points are shown in Figures 5 and 6, designated with a second arrow shift to higher values to correct for electron attachment.

Based on all of the above considerations, it is of interest to compare the most accurate indications of n_e from blunt probe σ_-, with n_e from Illinois nose-tip Ie data, and Illinois Faraday rotation and differential absorption points above 70 km. These are shown in Figures 7 and 8. While Figure 8 shows good agreement at all altitudes, this was an abnormal day. Figure 7 shows tip probe indications of n_e from I_e below 60 km to be lower than blunt probe n_e for σ_-; it is felt that the blunt probe technique and analysis is most accurate here. However, above 60 km, the blunt probe indications of n_e from σ_- are significantly lower than other diagnostics. Blunt probe methods above 65 km are approximate, and it is possible that these lower indicated densities are due to the approximate method of analysis used. These will be further explored in the future.

OUTGAS PERTURBATIONS OF MEDIUM SURROUNDING ROCKET BORNE PROBES

The primary concern in this work is with the intercomparison of electron density indicative diagnostics in the middle atmosphere. Particle collecting subsonic blunt probes and supersonic tip probes have been given detailed consideration, and the results of analyzing their data have been compared with other diagnostics. Generally speaking, those diagnostics are not sensitive to the presence of outgas material, since they function as collisional particle collectors and the mobility of electrons in outgas species would not generally inhibit collection. However, there are diagnostics that could be sensitive to the presence of outgas species, and so it is important to categorize the amount of outgas and the spatial distribution of outgas

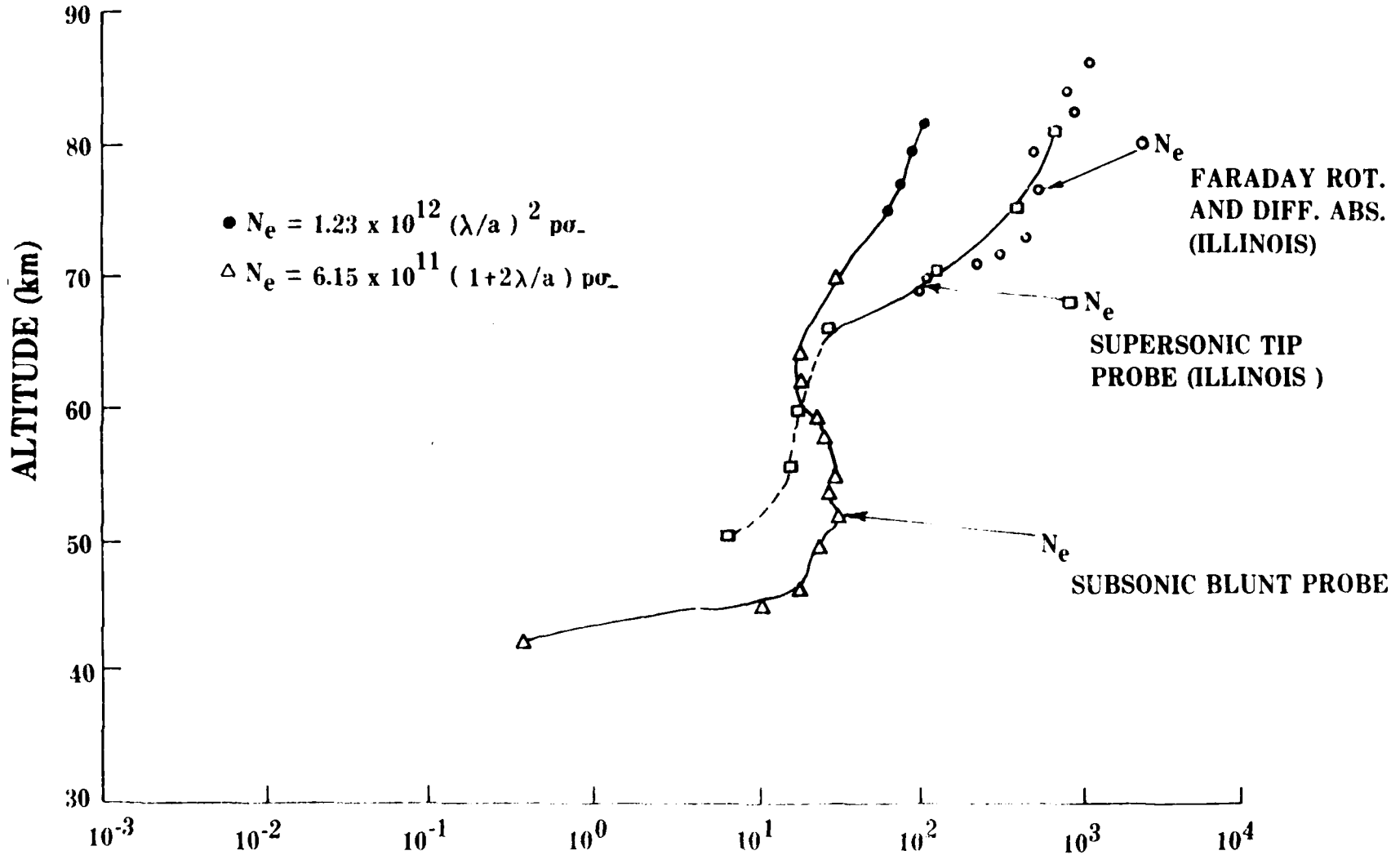

Figure 7. Electron density variations for January 31, 1972, 1230 EST, Wallops Island: from blunt probe, supersonic tip probe and local wave interaction methods.

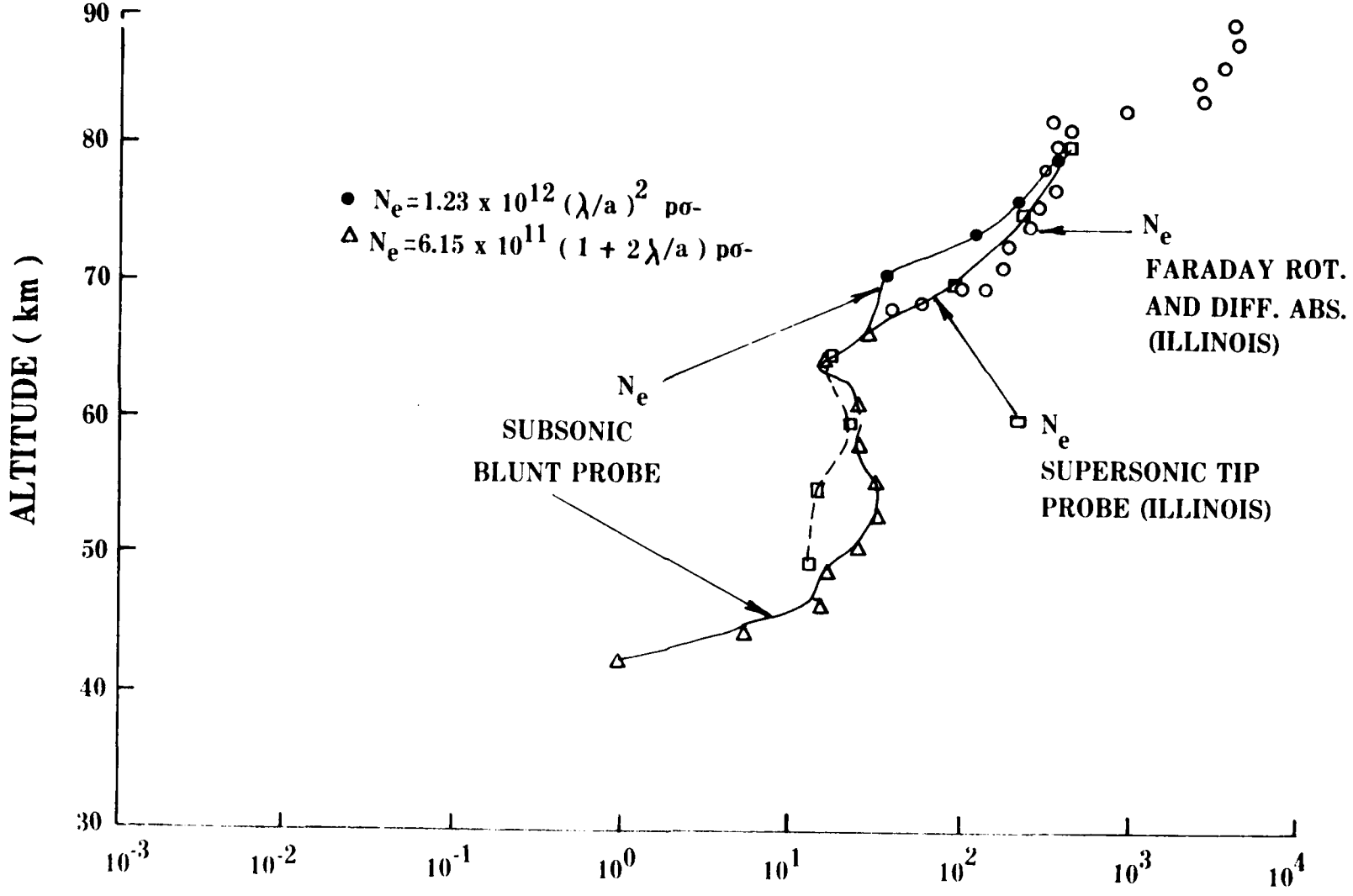

Figure 8. Electron density variations for December 5, 1972, 1230 EST, Wallops Island: from blunt probe, supersonic tip probe, and local wave interaction methods.

materials. In particular, one of the most important diagnostics for intercomparison purposes uses RF probe techniques.[7] The theory of these diagnostics has shown a dependence on electron collision frequency, and so consideration of outgas effects will be directed to that application. The work to be presented in this section will be a condensation of work that was informally reported earlier.[16]

Of particular interest here is the reported observation by Kendall[17] that, under the conditions of explosive decompression of the atmosphere surrounding a rocket-borne ionosphere probe, the rate of outgassing from the probe appears to be orders of magnitude larger than previously anticipated. Standard estimates[18] of outgas effects use rates that are more representative of conditions after pumping periods of hours or hundreds of hours. Accordingly, the composition of the gases near the surface of rocket-launched probes with a flight period of 5 to 10 minutes can be expected to be significantly different from earlier estimates. Since the gas desorbed by probe components is primarily water vapor, a natural component of the ionosphere whose density and chemical role is not well understood, any such species contamination is of considerable interest.

An attempt will be made here to estimate order-of-magnitude values of the water vapor density profiles near a desorbing probe surface so as to establish the extent of any distortion of ambient gas composition by the probe itself. The variation of concentration as a function of distance from a plane, outgassing surface will be considered.

The problem of determining the distribution of outgassing molecules near a solid-gas boundary involves consideration of the mass transfer at the boundary and the subsequent species diffusion; it possesses some similarity

to the problem of evaporation[19] (liquid-gas) and ablation[20] (solid-liquid-gas) in high temperature flows. The analysis of those two problems involves a coupling between mass and energy transfer, along with the required momentum balance in the situation with flow. The constraint normally applied at the boundary with the gas is the specification of equilibrium between the injected gas species (A) and the original gases present, i.e., the partial pressure of species A is the vapor pressure corresponding to the mixture pressure and temperature. Such a boundary condition is not meaningful in the outgas situation where the rate of molecules being introduced at the solid-gas surface is controlled by the mechanism of pressure imbalance between the surrounding gases and the adsorbed species, and is significantly influenced by the local surface physics.

A review of current understanding of the mechanisms involved in outgassing is presented by Santeler[21] et al. Briefly, a gas mixture in contact with a solid surface will, after a long period of time, reach a state of equilibrium where the amount of gas striking and adhering to the surface will equal the amount of gas leaving the surface. Absorption (surface) and absorption (volume) equilibrium will be reached. One possible model for the determination of surface partial pressure, while clearly approximate, may serve to indicate the surface-gas interaction in the outgas process.

In explosive decompression it may be assumed that loss of surface particles from adsorption will occur first. Accordingly, $q_L(0)$, the efflux of molecules (torr-liter/cm^2-sec) from the surface at t = 0 can be written as

$$q_L(0) = \frac{S_o}{\tau_R} = \alpha P_o (3.638) \sqrt{T/MW}$$

where S_o = quantity (number of molecules) of gas residing in a monolayer on the surface

τ_R = residence time of molecules in a monolayer on the surface (10 - 100 layers), sec

α = sticking fraction for molecules impinging on the surface

P_o = partial pressure of vapor in equilibrium at t = 0, torr

T = temperature, °K

M = molecular weight of the gas, gm/gm-mole

The above equation relates atomic surface properties (S_o, τ_R, α) with gas properties (P_o, T, MW). It is presumed that these (material) surface properties can be determined. Further, after the initiation of desorption, if it is assumed that the outgassed molecules will be lost at such a rate so as to establish a quasi-steady equilibrium with the wall, then

$$q_L(t) = \frac{S_o}{\tau_R} e^{-t/\tau_R} = P(3.638)\sqrt{T/MW} \quad .$$

This provides a possible scheme for determining the effective near-surface partial pressure (P) of the outgassed species as a function of time. While the accuracy of the above procedure clearly rests upon a precise knowledge of surface properties, it does serve to emphasize the relative independence of the surface boundary condition from either diffusion and/or flow effects. Models which preserve the dominance of such effects will now be examined.

TRANSIENT DIFFUSION INTO A SEMI-INFINITE MEDIUM

The physical problem being considered involves a solid with adsorbed gas being subjected to a surrounding gas pressure which will be decreased

from sea level atmosphere to effective vacuum over approximately a three-minute time period. The dynamic development of water vapor concentration profiles will be determined in a model where a plane solid is subjected to a vacuum ΔP increment at $t = 0$. The analysis of such a system is similar to that for evaporation of a liquid in a tube of infinite length[19] with 1-D diffusion. The basic solution is carried out for the case where the gas is maintained at constant pressure and temperature after initiation ($t = 0$). The solution is carried out in terms of dimensionless variables, as there is no characteristic length to be defined. With zero outgas concentration at $t = 0$ and z (normal distance) $= \infty$, the variation of outgassed species, is given by

$$\bar{X} = \frac{1 - \text{erf}(\bar{Z} - \phi)}{1 + \text{erf}\ \phi} \tag{1}$$

where $\bar{X} = X_A/X_{AO}$, $X_{AO} = X_A(z = 0)$

$\bar{Z} = z(4D_{AB}\ t)^{-1/2}$, z = distance from solid-gas interface

$X_A = \frac{C_A}{C}$, $C_A = \frac{\rho_A}{MW_A}\ (\frac{\text{mole}}{\text{cm}^3})$

$\phi = 1/C\ \sqrt{t/D_{AB}}\ N_{A_o}$

C = mixture concentration [$C = p/RT = \rho/MW$ (moles/cm^3)]

t = time (seconds)

D_{AB} = coefficient of mutual diffusion

N_{A_o} = flux of particles at $z = 0$ (gm-moles/cm^2-sec)

Thus, with a formula for D_{AB}, specification of p, T, z, t, N_{A_o} (outgas flux) will allow evaluation of ϕ; accordingly, the profile of X_A/X_{A_o} can be determined. However, since no boundary condition or composition has been specified, both $X_A(z,t)$ and $X_{A_o}(t)$ are unknown.

It should be noted that in the form presented above, the solution is exact only for small values of X_A i.e., where outgas species A is diffusing through a background species, B. In order to place the solution in perspective, one calculation of interest involves the determination of the distance from the wall within which 90 percent of the outgas mass is contained i.e., where $X_A/X_{A_o} = 0.1$; for convenience, we call this distance $z(0.1)$. As a simplifying assumption, a linear variation of composition is utilized in some integrations to arrive at a closed form expression,

$$z(0.1) = 2.3 \sqrt{D_{AB}} \; t^{1/2} + 2 \frac{N_{A_o}}{C} t$$

Following Bird, Steward, and Lightfoot,[19]

$$D_{AB}\left(\frac{cm^2}{sec}\right) = \frac{2}{3}\left(\frac{k}{\pi}\right)^{3/2} \left\{\frac{1}{2m_A} + \frac{1}{2m_B}\right\}^{1/2} \frac{T^{3/2}}{p(d_A + d_B/2)^2}$$

so at 50 km, $D_{AB} = 4.1 \times 10^2$ cm^2/sec, and $C(50\ km) = 3.5 \times 10^{-8}$ gm-mole/cm.^{3} Using the outgas rate indicated by Kendall[17] (worst case, anodized aluminum) $N_{A_o} = 1.7 \times 10^{-8}$ gm-moles/cm^2-sec, then for

$t = 10^{-2}$ sec , $\quad z(0.1) = 4.6$ cm

$t = 1$ sec , $\quad z(0.1) = 48$ cm

Diffusion of outgas species will proceed to a steady state distribution in a time period short compared with the characteristic time of the local probing event ($\sim$ 1 sec). Alternatively, it can be stated that the diffusion length scale will considerably exceed the scale of the probe geometry. Accordingly, in the present case the diffusion can be treated as steady state and so will be controlled by probe and flow generated dimensions and boundary conditions.

STEADY STATE DIFFUSION THROUGH A BOUNDARY LAYER

The model chosen is normally used to represent diffusion through a tube from which particles are carried away ($\bar{X}_A = 0$) at one end ($z = z_2$) by a gas flow perpendicular to the direction of diffusion. Such a model can be used to represent the diffusion of outgassed vapor in a case with flow impingement, if an appropriate length scale can be selected to represent the distance from the boundary within which the flow will not disturb the diffusion. Such a dimension can be defined and related to a boundary layer thickness.

As outlined in the literature[19] the diffusive flux of A particles through medium B can be expressed by

$$N_A(Z) = - \frac{CD_{AB}}{1 - X_A} \frac{dX_A}{dZ} ; \quad X_A = \frac{C_A}{C} , \quad C_A = \frac{\rho_A}{MW_A}$$

with the boundary conditions

$$N_{outgas} = N_{A_o} \left(\frac{gm\text{-}mole}{cm^2\text{-}sec}\right) \quad at \quad z = z_1 = 0$$

$$X_A = 0 \quad at \quad z = z_2 ,$$

This equation can be integrated to predict the concentration ratio at the surface as

$$X_{A_o} = 1 - e^{-\{N_{A_o}/D_{AB} \cdot C\}z_2}$$

Determination of outgas species distribution in the case with flow impingement presents a complex problem. The velocity flow field can be separated into two regions: (1) an inviscid (external) flow region and (2) flow within a viscous boundary layer. The thickness of the boundary

layer presents a natural length with which to scale the flow problem. Specifically,[19] with laminar flow along a flat plate, and the outgas of species A at the plate with concentration C_{A_o}, the A species will diffuse and have non-zero concentration within a diffusion layer of thickness, δ_D, approximately specified as

$$\Lambda = \frac{\delta_D}{x} \propto (Sc)^{-1/3} = \left(\frac{\nu}{D_{AB}}\right)^{1/3}$$

The absence of chemical reactions is presumed. Evaluating the above parameter for a specific altitude, $\Lambda(50\ km) = 1.33$, so the viscous boundary layer thickness provides a reasonable representation of the region within which outgassed molecules will be distributed along a flat plate. While the stagnation region of a flow normal to a flat plate is of some interest here, these results for flow along a flat plate also provide a relevant length scale for stagnation boundary flow.

Fundamentally, the flow field near the approximately plane boundary will always be subsonic in nature, since even with supersonic flow, a normal shock wave will convert the incoming supersonic flow to subsonic flow, with a density higher than ambient behind the shock. The incompressible stagnation region is considered by Schlichting[22] where the thickness of the axisymmetric boundary layer is given as

$$\delta = 2.8\sqrt{\nu/2a} \quad \text{where } a = du/dr\ , \quad \nu = \mu/\rho$$

For a flat-nosed, right-circular cylinder

$$a = \frac{4U}{D} \qquad \text{with } U = \text{free stream velocity and}$$

$$D = \text{diameter of cylinder}$$

and directly, with U = 100 m/sec, D = 0.1 m,

$$\delta(50\ \text{km}) = 0.65\ \text{cm}$$

$$\delta(70\ \text{km}) = 2.0\ \text{cm}$$

$$\delta(90\ \text{km}) = 11.0\ \text{cm}$$

With an appeal to the "similarity" of flow within the boundary layers of tangent and normal flat plate flows, the approximation that the concentration of outgas molecules will be effectively zero at the outer edge of the diffusive and viscous boundary layer thickness can be made, and an order of magnitude for the surface concentration of the outgas species can be arrived at. Presuming steady state diffusion with no mass build-up through a boundary layer thickness, the relationship for concentration of outgas species at the surface is:

$$\frac{C_{A_o}}{C} = 1 - e^{-\{N_{A_o}/CD_{AB}\} \cdot \delta_D}$$

With $N_{A_o} = 1.7 \times 10^{-8}$ gm-moles/cm^2-sec, $\delta = \delta_D$, then $C_{A_o}/C \approx 10^{-3}$. At 50 km, the indicated density of water vapor at the surface is $n_{H_2O} = 2 \times 10^{12}/\text{cm}^3$, one to two orders of magnitude higher than the water vapor density in the ambient, undisturbed atmosphere.

Based on the above calculations, consideration will now be given to the influence of outgas water vapor on electron density diagnostics with the impedance probe.

INFLUENCE OF OUTGAS SPECIES ON THE REDUCTION OF ELECTRON DENSITIES FROM IMPEDANCE PROBE MEASUREMENTS

The use of RF probing techniques for the determination of electron densities has been accepted over a period of years.[7] One early work

satisfactorily compared the general performance behavior of three different techniques: (1) the standing wave impedance probe or impedance probe; (2) the plasma frequency probe or plasma probe; and (3) a resonance rectification probe. The analysis of the interactions occurring with each of these types of diagnostics was reviewed in some detail by Despain.[23] An attempt at quantitative comparison of n_e from impedance probes and the other diagnostics was reported by Ulwick[24] in relation to data gathered during a solar particle event (PCA 69). However, these n_e indications were not absolute and the altitudes of best accuracy were from 80 km to 125 km. An attempt at intercomparison of an RF probe, the plasma frequency type, with a DC Langmuir probe was carried out by Kotadia and Kist[25] who reported reasonable agreement of measurements taken from 95 to 150 km.

Basic analyses of RF interactions with plasmas have been presented by a number of authors, and in some cases experiments have been reported. Specifically, Balmain[26] presented a basic theory and some confirming laboratory experiments with a cylindrical antenna. Sheath effects and collisions were more accurately modeled in a later work,[27] but in general, most interest was focused toward plasma frequency diagnostics. A spherical impedance probe was evaluated in a laboratory experiment by Tarstrup and Heikkila,[28] who examined fluid effects and effects of electron-neutral collision frequency. Again, conditions near plasma frequency were most important. A later work[29] examined transient sheath effects. A reasonably comprehensive analysis of the impedance of a spherical probe in a warm plasma, with collision effects, was presented by Aso.[30] In almost all of the works noted above, the emphasis was directed toward exploring behavior near plasma frequency.

A somewhat different emphasis is involved in the impedance probe application as outlined by Despain.[23] The impedance probe technique generally functions with ω, the operating or driving frequency, being lower than the plasma frequency. The impedance probe is used to determine values of electron density, electron temperature, and collision frequency from the difference between values of the impedance in plasma and in vacuum. Computer developed solutions for resistance and reactance typically have been generated and graphed as a function of plasma frequency and temperature for different values of collision frequency. It will be noted that the primary effect of electron collisions in the approximate calculation procedures developed by Despain[23] is to increase the antenna resistance.

The data gathered by the impedance probe allows the determination of the difference of the antenna impedance from free space impedance, or

$$\Delta\bar{Z} = \Delta R - i\,\Delta\bar{X}$$

where R is the resistance and $\bar{X}$ is the reactance component of the impedance. Based on analysis of an equivalent circuit for the probe, the following equations have been developed

$$\Delta R = \frac{\bar{X}\, Z}{\omega\, C_o[(1 - \bar{X})^2 + Z^2]}$$

$$\Delta\bar{X} = \frac{\bar{X}(1 - \bar{X})}{\omega\, C_o[(1 - \bar{X})^2 + Z^2]}$$

where $\bar{X} = \omega_p^2/\omega^2$, $\omega_p^2 = (n_e\, e^2/m_e\, \epsilon_o)$, $Z = \nu/\omega$ where ν is electron collision frequency, $C_o = C_1 + C_2$ where C_o is the shunt capacitance of the

antenna mount and C_o is the free space capacitance of the antenna. In straightforward fashion,

$$\bar{X} = \frac{C_2 \omega^2}{\epsilon_o \omega^2} \frac{p}{} = \frac{\omega C_o [\Delta\bar{X} + (\Delta R)^2/\Delta\bar{X}]}{1 + \omega C_o [\Delta\bar{X} + (\Delta R)^2/\Delta\bar{X}]}$$

$$= \frac{\Delta R/\Delta\bar{X}}{1 + C_o [\Delta\bar{X} + (\Delta R)^2/\Delta\bar{X}]}$$

These two equations deserve careful examination. First, [illegible] n_e and ν can be carried out with [illegible] data, [illegible] model of the ionosphere. That is, the presence of [illegible] material will have no effect on n_e or ν in this procedure. [illegible], the only accurate test of this method would involve the comparison of ν and ν so determined with independent, accurate n_e and ν values. [illegible] comparison of ν using this technique is not known to the authors, one point can be made that, in general, n_e values derived from this technique are higher than those from other diagnostics. The ultimate test of the method, intercomparison, does seem to imply a difficulty with the technique. Differences between n_e upleg and downleg have been rationalized in the past as being due to outgas,[8] and so it is natural to examine the possible influence of outgas effects.

First, the functional forms for ΔR (resistance) and ΔX (reactance) demonstrate opposing effects due to collision. Consider the determination of $\bar{X}$ from ΔR, C_o, Z or $\Delta\bar{X}$, C_o, Z. For a given value of $\Delta\bar{X}$, inclusion of outgas enhanced collision effects would indicate a larger n_e than without collision effects. For a given value of ΔR, however, inclusion of outgas enhanced collision effects would indicate a smaller n_e than without collision

effects, Recall, however, that the scheme for computation of n_e does not directly include a collisional model. Without a new fundamental development of impedance relationships, it is not clear whether the approximate method of n_e determination outlined by Despain is internally self consistent with respect to collision frequency. Rather than to judge the accuracy of that technique with respect to collision frequency effects on n_e determination, present efforts will concentrate on defining physical behavior of the probe and then indicating how collision effects could influence the determination of n_e. Again, collision effects produce a dominant effect on the real component of impedance, the resistance. This is consistent with physical understanding of the effects of electron collisions, i.e., there is a direct reduction of effective conductivity of a medium with increased ν, and so a direct reduction of signal amplitude. Changes in phase are directly related to reactance changes, and such measurements can be more troublesome to interpret. Specifically, if one takes the formula for $\bar{X}$ as a function of ΔR and $\Delta\bar{X}$, there would be no effect on n_e due to outgas. If one would take the formula for $\Delta\bar{X} = f(\bar{X}, Z)$, again, there is little effect on n_e determination due to Z. However, if one would take the formula for $\Delta R = f(\bar{X}, Z)$ and use it to determine n_e, there would be definite changes in indicated n_e due to the presence of outgas material. Some details will now be outlined.

The effects of outgas will manifest themselves directly in the collision frequency, which can be written

$$\nu_{en} = \left(\frac{8}{\pi}\right)^{1/2} \left(\frac{kT_e}{m_e}\right)^{1/2} \sum_j n_j Q_{ej}$$

where Q_{ej} is the collision cross section. For the altitudes of interest, the gases are primarily N_2, so we can write

$$\nu_{en}(\sec^{-1}) = \left(\frac{8}{\pi}\right)^{1/2}\left(\frac{kT_e}{m_e}\right)^{1/2} \left\{ [N_2]Q_{eN_2} + [H_2O]Q_{eH_2O} \right\}$$

Typical values[31] are $Q_{eN_2} \approx 4 \times 10^{-16}$ cm^2 and $Q_{eH_2O} \approx 10^{-13}$ cm^2 and the basis for any sensitivity to outgas can be seen to reside in the collision cross section which is a factor of 10^3 higher than that for N_2. In order to gauge effects of outgas in this fashion, the calculations noted above will be used: a constant value of $f \equiv [H_2O]/[N_2] = .004$ will be used for all altitudes. In order to estimate the electron density in the undisturbed medium (without outgas or shock compression), several steps must be taken. Values of electron density that have been provided were deduced by straightforward application of $\bar{X} = f(\Delta R, \Delta\bar{X})$. However, since the rocket is flying supersonically, correction will first be made to these values of n_e to account for both shock compression and electron attachment effects (as was done for the supersonic Langmuir tip probe) to attempt to recover undisturbed electron density. These will be presented in graphical form to indicate the magnitude of corrections. A second procedure to account for outgas effects will then be carried out. It initiates by computing ΔR from $\bar{X}$. The effects of outgas are included by incorporating Z into the $\bar{X} = f(\Delta R, Z)$ formula to get a new (reduced) n_e value. Finally, as above, the effects of shock compression and electron attachment are also accounted for to recover undisturbed n_e, in this second case with corrections for outgas and shock effects.

As a sample calculation, and it must be emphasized that data from a single day is limited in usefulness, one day on which comparisons of n_e could

be made from a number of diagnostics will be considered. Data were recorded for intercomparison purposes by a number of diagnostics on a day preceding the eclipse, but part of the 1979 Canada-US Solar Eclipse Program. Specifically, data were recorded by a blunt probe flown by Mitchell (UTEP), supersonic Langmuir tip probe data and impedance probe data was recorded by E. Pound (USU), partial reflection data were recorded by R. O. Olsen (WSMR) and reduced by D. Mott (NMSU). The presentation of calculated electron densities from this preliminary data is first made in Figure 9. The blunt probe, tip probe, and partial indications of n_e have been made based on the methods noted above. The Langmuir tip probe data was corrected for shock wave and attachment effects with an x15 attachment enhancement factor. The impedance probe data (ascent and descent) is presented first without any adjustment; second, with adjustment for shock wave compression and attachment effects; third for outgas adjustment with f = 0.004 added to the shock and attachment effects.

The presentations of calculated electron densities including all the effects and techniques noted above are given in Figure 10. For this particular day, generally, there does appear to be reasonable agreement between supersonic nose-tip Langmuir probe indications of n_e and those from the impedance probe. Both these diagnostics which were on the same vehicle do differ above 65 km from the n_e values deduced from blunt probe data and partial reflection data. It is noted above that blunt probe analysis above 65 km is questionable and could give n_e values that are up to an order of magnitude low at 75 km. Also, the inversion of the partial reflection profile above 65 km is a typical output when the technique ceases to provide accurate n_e values. However, these were very active days and, as n_e point, the interval of time

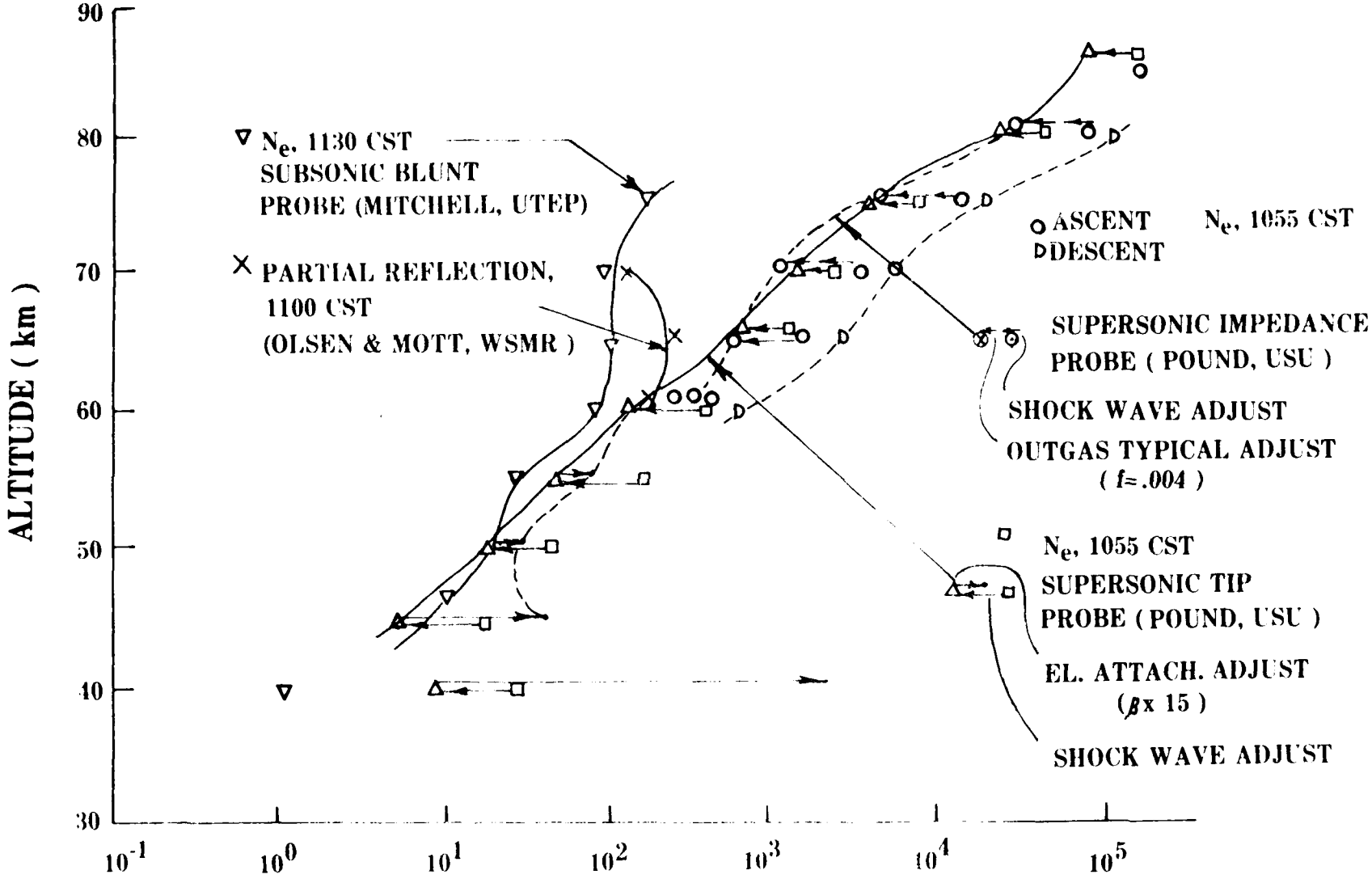

Figure 9. Comparisons of detailed calculations of electron density variations for February 24, 1979, Red Lake (preliminary).

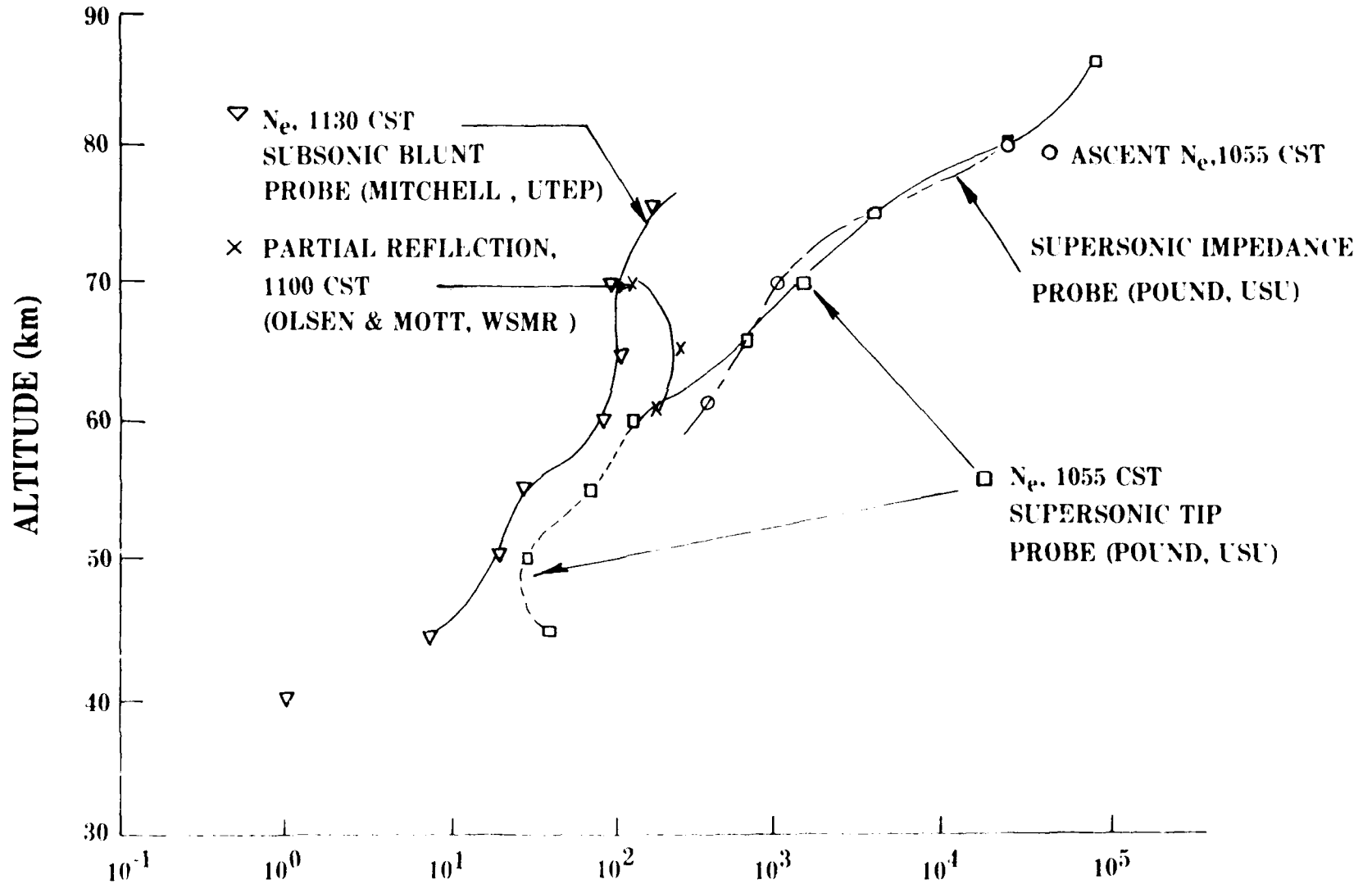

Figure 10. Comparison of calculated electron density variations for February 24, 1979, Red Lake.

between the blunt probe data shot (1130 CST) and the second shot with the impedance and tip probe (1055 CST) could be responsible for the differences that are evident.

REFERENCES

1. D. W. Hoock and M. G. Heaps, "DAIR CHEM: A computer code to model ionization-deionization processes and chemistry in the middle atmosphere," Users Manual, Atm. Sci. Lab., White Sands Missile Range, N. M., March 1978.

2. W. Swider, "Electron concentrations in the C-region," Paper SA10, AGU 1979 Fall Meeting, San Francisco, Calif., December 1979.

3. "The upper atmosphere and magnetosphere," The Geophysics Study Committee, National Research Council, National Academy of Sciences, Washington, D.C., 1977.

4. C. F. Sechrist, Jr., "Comparison of techniques for measurement of D-region electron densities," Radio Science, Vol. 9, pp. 137-149, 1974.

5. E. A. Mechtly, "Accuracy of rocket measurements of lower ionosphere electron concentrations," Radio Science, Vol. 9, pp. 373-378, 1974.

6. H. G. Booker and E. K. Smith, "A comparative study of ionospheric measurement techniques," J. Atm. Terr. Phys., Vol. 32, pp. 467-497, 1970.

7. K. D. Baker, A. M. Despain and J. C. Ulwick, "Simultaneous comparison of RF probe techniques for determination of ionospheric electron density," J. Geophys. Res., Vol. 71, pp. 935-944, 1966.

8. J. C. Ulwick, "Comparison of black brant rocket measurements of charged particle densities during solar particle events," Proc. of COSPAR Symposium on the Solar Particle Event of November 1969, in AFCRL 72-0474, SR No. 144, Air Force Cambridge Research Lab., August 11, 1972.

9. N. C. Maynard, Ed., "Middle atmosphere electrodynamics," NASA-CO-2090, June 1979.

10. T. M. York, "Measurement of electron densities in the middle atmosphere using rocket-borne blunt probes," Atm. Sci. Lab., Report CR-79-0109-5, White Sands Missile Range, October 1979.

11. T. M. York, R. O. Olsen, J. D. Mitchell and D. L. Mott, "Evaluation of electron densities in the middle atmosphere using rocket borne blunt probes," submitted for publication in J. Atm. Terr. Phys., January 1980.

12. T. M. York, C. I. Wu, T. W. K. Lai, "Electron collection by blunt electrostatic probes used in measurements of the lower ionosphere," AIAA Paper 79-1541, July 1979.

13. A. H. Shapiro, The Dynamics and Thermodynamics of Compressible Fluid Flow. Vol. II, The Ronald Press Company, New York, 1954.

14. J. D. Mitchell, "An experimental investigation of mesospheric ionization," Report PSU-IRL-SCI-416, Ionosphere Research Laboratory, The Pennsylvania State University, University Park, Pa., 1973.

15. M. G. Heaps, "The 1979 solar eclipse and validation of D-region models," Report ASL-TR-0002, Atmospheric Sciences Laboratory, White Sands Missile Range, N.M., 1978.

16. T. M. York, "Outgassing from rocket-borne ionosphere probes--Evaluation of near surface composition and comparison with atmospheric water vapor concentrations," Rept. PSU-IRL-IR-17, Ionosphere Research Laboratory, Pennsylvania State University, December 1972.

17. B. R. F. Kendall and J. O. Weeks, "Transient desorption of water vapor: A potential source of error in upper atmosphere rocket experiments," J. Geophys. Res., Vol. 79, pg. 1592, 1974.

18. B. B. Dayton, "Outgassing rates of contaminated metal surfaces," Trans. 8th Nat. Vac. Symp. and 2nd Int. Conf. on Vac. Sci. and Tech., Vol. I, L. E. Preuss, Ed., Pergamon, 1962.

19. R. B. Bird, W. E. Stewart and E. N. Lightfoot, Transport Phenomena, John Wiley and Sons, Inc., New York, 1960.

20. W. H. Dorrence, Viscous Hypersonic Flow, McGraw-Hill, 1962.

21. D. J. Santeler, et al., Vacuum Technology and Space Simulation, NASA SP-105, Washington, 1966.

22. H. Schlichting, Boundary Layer Theory, 4th Ed., McGraw-Hill, 1960.

23. A. M. Despain, "Antenna impedance in the ionosphere," Space Science Laboratory Report, Utah State University, Logan, Utah, November 1970.

24. J. C. Ulwick, "Comparison of black brant rocket measurements of charged particle densities during solar particle events," AFCRL 72-0474, SR No. 144, Air Force Cambridge Research Lab, August 11, 1972.

25. K. M. Kotadia and R. Kist, "Comparison of electron density profiles obtained by DC and RF probes," Space Research, Vol. 17, Proc. of COSPAR Symposium, Philadelphia, Pa, 1976.

26. K. G. Balmain, "The impedance of a short dipole antenna in a magneto-plasma," IEEE Trans. on Antennas and Propagation, Vol. 15, pp. 605-617, 1964.

27. K. G. Balmain, "Impedance of a radio-frequency plasma probe with an absorptive surface," Radio Science, Vol. 1, pp. 1-12, 1966.

28. J. Tarstrup and W. J. Heikkila, "The impedance characteristic of a spherical probe in an isotropic plasma," Radio Science, Vol. 7, pp. 493-502, 1972.

29. W. D. Bunting, Jr. and W. J. Heikkila, "Transient ion sheath effects on probe admittance," J. Appl, Phys., Vol. 42, pp. 1136-1144, 1971.

30. T. Aso, "Impedance of an ion-sheathed spherical probe in a warm, isotropic plasma," Radio Science, Vol. 8, pp. 139-146, 1973.

31. E. W. McDaniel, Collision Phenomena in Ionized Gases, John Wiley and Sons, Inc., New York, 1964.

END

DATE
FILMED

1 81

DTIC